Inorganic Materials, Vol. 40, No. 8, 2004, pp. 867–873. Translated from Neorganicheskie Materialy, Vol. 40, No. 8, 2004, pp. 993–1000.

Effect of Synthesis Conditions on the Lithium Nonstoichiometry and Properties of $La_{2/3-x}Li_{3x}\square_{4/3-2x}M_2O_6$ (M = Nb, Ta) Perovskite-like Solid Solutions

A. G. Belous, O. N. Gavrilenko, E. V. Pashkova, K. P. Danil'chenko, and O. I. V'yunov

Institute of General and Inorganic Chemistry, National Academy of Sciences of Ukraine, pr. Akademika Palladina 32/34, Kiev, 03142 Ukraine

e-mail: belous@ionc.kar.net

Received July 11, 2003; in final form, November 13, 2003

Abstract—The effects of the nominal composition and synthesis conditions on the lithium nonstoichiometry of $La_{2/3-x}Li_{3x}\square_{4/3-2x}Nb_2O_6$ (I) and $La_{2/3-x}Li_{3x}\square_{4/3-2x}Ta_2O_6$ (II) solid solutions are studied. The results demonstrate that lithium losses can be reduced from 26–30 to 14–15 mol % in system I and from 15 to 4 mol % in system II. It is shown that the disturbance of electroneutrality caused by Li nonstoichiometry in the solid solutions is eliminated via the formation of oxygen vacancies in positions O(1) (1*f*: 1/2 1/2 0) and O(2) (1*h*: 1/2 1/2 1/2) of the cation-deficient perovskite structure. The optimal lithium ion conductivity is offered by solid solutions with $\square/3x \simeq 2.6$ and $x \simeq 0.136$–0.143.

INTRODUCTION

Partial replacement of La^{3+} by $3Li^+$ in $La_{2/3}\square_{1/3}TiO_3$, first proposed in [1], has recently received considerable attention, motivated by the search for new cation conductors [2–8]. Of particular interest are $La_{2/3-x}Li_{3x}\square_{4/3-2x}M_2O_6$ (M = Nb, Ta) A-site deficient perovskites [4–7], whose structure is shown schematically in Fig. 1. The presence of vacancies and tetragonal channels in the structure of $La_{2/3-x}Li_{3x}\square_{4/3-2x}M_2O_6$ (M = Nb, Ta) [9] is favorable for ionic transport. According to Emery *et al.* [2], sintering of $(La_{2/3-x}Li_{3x}\square_{1/3-2x})TiO_3$ may cause lithium losses up to 30%. Mirumoto and Hayashi [4] reported that sintering of $La_{2/3-x}Li_{3x}Ta_2O_6$ samples embedded in powder of nominal composition was accompanied by lithium losses of 8%. At the same time, in most studies of these solid-solution systems the results were interpreted with no allowance for lithium losses. A literature search revealed no works aimed at identifying the factors influencing the Li loss during the synthesis of lithium ion conducting cation-deficient perovskites and the process steps in which the largest lithium losses occur. Clearly, the lack of such data is a serious impediment to controlled synthesis of the materials in question.

The objective of this work was to investigate the effect of synthesis conditions on the lithium nonstoichiometry and transport properties of $La_{2/3-x}Li_{3x}\square_{4/3-2x}Nb_2O_6$ (I) and $La_{2/3-x}Li_{3x}\square_{4/3-2x}Ta_2O_6$ (II) perovskite solid solutions and to find ways of reducing lithium losses.

EXPERIMENTAL

$La_{2/3-x}Li_{3x}\square_{4/3-2x}M_2O_6$ samples with $x = 0.17$–0.42 were prepared by solid-state reactions (SRs), as described previously [10–12], using LO-1 La_2O_3 and extrapure-grade Nb_2O_5, Ta_2O_5, and Li_2CO_3 as starting chemicals. $La_{0.5}Li_{0.5}M_2O_6$ ($x = 0.17$) samples were also prepared via hydroxide coprecipitation (HC) and by topotactic reactions (TRs), using presynthesized $LiNbO_3$, $LiNb_3O_8$, and $LaNbO_4$ [13]. Lanthanum and niobium (tantalum) hydroxides were coprecipitated by adding a 25% aqueous solution of NH_4OH to a mixture of ethanolic solutions of $La(NO_3)_3$ and MCl_5 at pH 9. The reaction was left standing for 24 h. Next, the precipitate was washed and, after adding an appropriate amount of aqueous LiOH, the solution was boiled down on a sand bath. The subsequent steps were similar to those in SRs [10–12].

Prior to the synthesis of samples I with $x = 0.17$ by TRs, we prepared $LiNbO_3$, $LiNb_3O_8$, and $LaNbO_4$ by firing stoichiometric oxide–carbonate mixtures at 1220 (2 h), 1220 (2 h), and 1420 K (1 h), respectively. $LaNbO_4 + LiNbO_3 + Nb_2O_5$ and $LaNbO_4 + LiNb_3O_8$ mixtures were reacted at 1320 K for 1.5 h, and the resultant powders were pressed and then sintered at 1480 K.

X-ray diffraction (XRD) measurements were made on a DRON-4-07 powder diffractometer (CuK_α radiation, $2\theta = 10°$–$150°$, step-scan mode with a step size of $\Delta 2\theta = 0.02°$ and a counting time per data point of 10 s).

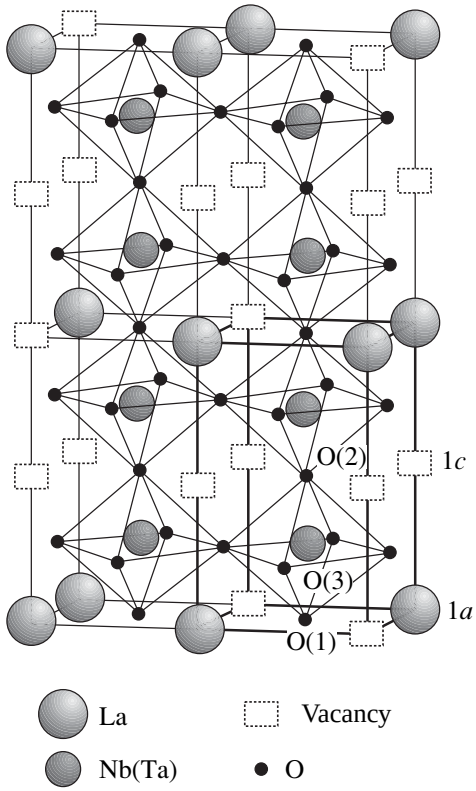

Fig. 1. Structure of the cation-deficient perovskites $La_{2/3}\square_{4/3}M_2O_6$ (M = Nb, Ta). La (1*a*: 0 0 0), Nb (2*t*: 1/2 1/2 *z*), O(1) (1*f*: 1/2 1/2 0), O(2) (1*h*: 1/2 1/2 1/2), O(3) (2*s*: 1/2 0 *z*), O(4) (2*r*: 0 1/2 *z*), vacancies (1*c*: 0 0 1/2).

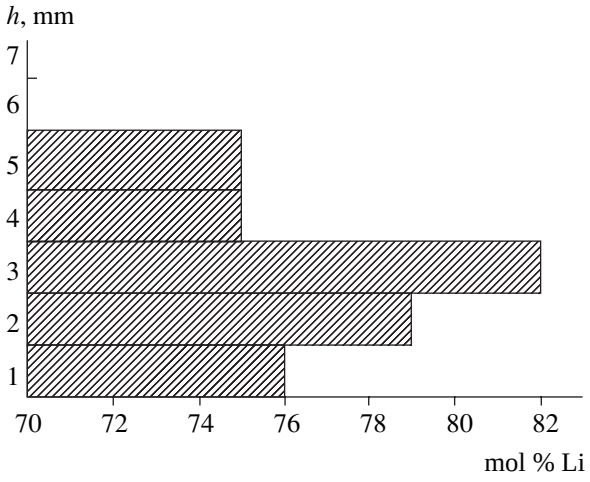

Fig. 2. Lithium distribution (molar percent relative to the nominal composition $La_{0.5}Li_{0.5}Nb_2O_6$) in the height direction of a sintered sample.

As external standards, we used SiO_2 and Al_2O_3 (NIST SRM1976 standard [14]). Structural parameters were refined by the Rietveld profile analysis method. Electrical conductivity was measured as described elsewhere [12] with an accuracy of ±15–20%. The lithium content of the samples was determined by atomic absorption on a Pye Unicam SP9 spectrophotometer, using an air–acetylene flame. The detection limit was 0.02 mg/l. Polycrystalline samples for atomic absorption analyses were dissolved as described in [15].

RESULTS AND DISCUSSION

According to earlier studies [10–12], the solid-solution ranges in systems I and II are x = 0–0.25. Table 1 summarizes the atomic absorption data for systems I

Table 1. Atomic absorption data $La_{2/3-x}Li_{3x}\square_{4/3-2x}M_2O_6$ samples prepared by SRs (Li content as a function of nominal composition)

Sample no.	Nominal composition			Actual composition, $La_{2/3-x}Li_{3x}\square_{4/3-2x}Nb_2O_6$		Actual composition, $La_{2/3-x}Li_{3x}\square_{4/3-2x}Ta_2O_6$	
	3*x*	*x*	□	3*x*	Li losses, mol %	3*x*	Li losses, mol %
1	0.32	0.106	1.12	0.21 (0.22–0.20)	37 (38–36)	–	–
2	0.38	0.126	1.08	–	–	0.30 (0.31–0.29)	21 (19–23)
3	0.50	0.166	1.00	0.37 (0.40–0.34)	26 (20–32)	0.42 (0.44–0.40)	15 (12–18)
4		Powder*					
	0.50	0.166	1.00	0.40 (0.42–0.38)	20 (15–25)		
5		Compact*					
	0.50	0.166	1.00	0.39 (0.42–0.36)	21 (15–27)		
6	0.62	0.206	0.92	–	–	0.56 (0.57–0.55)	12 (11–13)
7	0.74	0.246	0.84	0.56 (0.57–0.55)	24 (23–25)	0.68 (0.69–0.67)	11 (9–13)

Note: Figures in parentheses indicate the scatter in 3*x*.
* Li content was determined after firing at 1320 K.

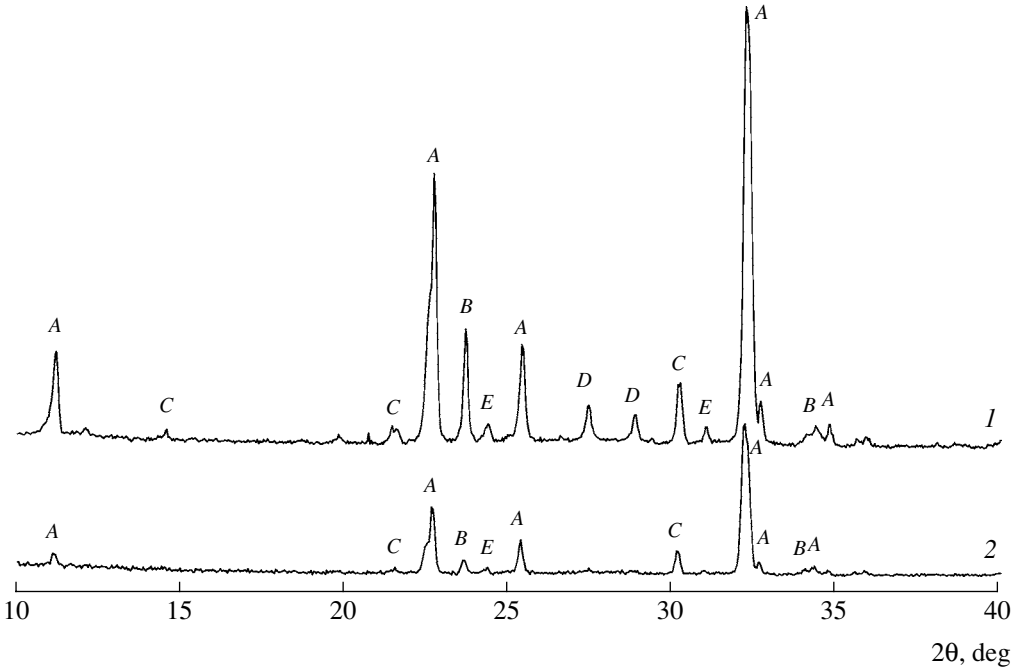

Fig. 3. XRD patterns from $La_{0.5}Li_{0.5}Nb_2O_6$ samples annealed at 1320 K for 2 h: (*1*) powder, (*2*) compact; *A* = cation-deficient perovskite, *B* = $LiNbO_3$, *C* = $LiNb_3O_8$, *D* = $LaNbO_4$, *E* = Nb_2O_5.

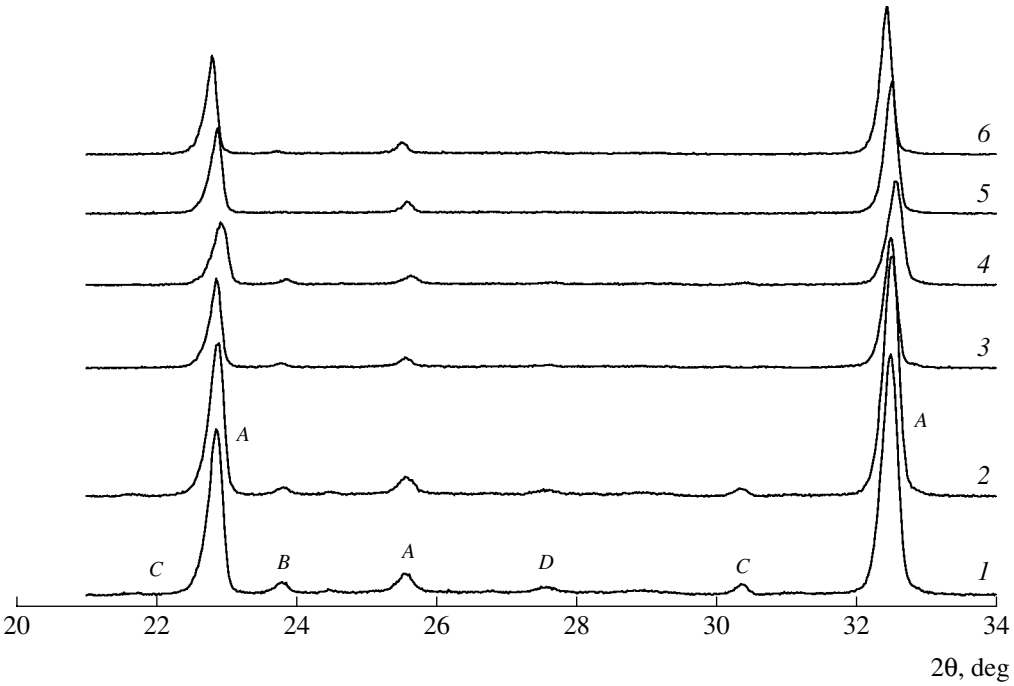

Fig. 4. Portions of the XRD patterns from $La_{0.5}Li_{0.5}Nb_2O_6$ calcined at 1420 K for (*1*) 5, (*2*) 15, (*3*) 30, (*4*) 60, (*5*) 240, and (*6*) 300 min; *A* = perovskite, *B* = $LiNbO_3$, *C* = $LiNb_3O_8$, *D* = $LaNbO_4$.

and II: Li content as a function of nominal composition within the solid-solution range. In systems I and II, the lithium losses decrease with increasing nominal lithium content ($3x$), presumably because the Li^+ mobility decreases with decreasing vacancy concentration. Figure 2 illustrates the Li distribution in the height direction for a sintered pellet. The lithium loss is 18 mol % in the center part of the pellet and 25–26 mol % in the surface layers. According to earlier results [13, 16], heat treatment of La_2O_3 + Li_2CO_3 + M_2O_5 mixtures

Table 2. Effect of synthesis conditions on the lithium content of $La_{2/3-x}Li_{3x}\square_{4/3-2x}MO_6$ ceramics with $x = 0.17$

Method	Sample no.	Synthesis conditions					ρ, g/cm^3	Li content after sintering	Li losses, mol %
		Precursor mixture	T_{ann}, K	τ_{ann}, h	T_{sint}, K	τ_{sint}, h		3x	
SR	*1*	$0.25La_2O_3$–$0.25Li_2CO_3$–Nb_2O_5	1320	2	1490	1	5.07	0.37 (0.40–0.34)	26
	2	$0.25La_2O_3$–$0.25Li_2CO_3$–Ta_2O_5	1320	2	1770	1	7.35	0.42 (0.44–0.41)	15
	3	$0.25La_2O_3$–$0.29Li_2CO_3$–Nb_2O_5	1320	2	1480	1	5.27	0.33 (0.36–0.30)	42, 34*
	4	$0.25La_2O_3$–$0.33Li_2CO_3$–Nb_2O_5	1320	2	1460	1	5.14	0.37 (0.40–0.34)	44, 26*
	5	$0.25La_2O_3$–$0.36Li_2CO_3$–Nb_2O_5	1320	2	1450	1	5.07	0.39 (0.42–0.36)	46, 22*
	6	$0.25La_2O_3$–$0.25Li_2CO_3$–Nb_2O_5	970 + 1320	4 + 1.5	1490	1	5.21	0.42 (0.46–0.38)	15
TR	*7*	$0.5LaNbO_4$–$0.5LiNbO_3$–$0.5Nb_2O_5$	1320	1.5	1480–1490	1	4.98	0.44 (0.46–0.42)	11
	8	$0.5LaNbO_4$–$0.5LiNb_3O_8$	1320	1.5	1480–1490	1	5.19	0.43 (0.44–0.42)	14
HC	*9*	$0.5La(OH)_3$–$0.5LiOH$–$2Nb(OH)_5$	1320	1.5	1450	1	4.97	0.37 (0.38–0.36)	26
	10	$0.5La(OH)_3$–$0.5LiOH$–$2Ta(OH)_5$	1320	1.5	1670	1	7.43	0.48 (0.49–0.47)	4

Note: T_{ann}, τ_{ann}, T_{sint}, and τ_{sint} are the annealing and sintering temperatures and durations; figures in parentheses indicate the scatter in 3x.
* Losses relative to the nominal composition.

may give rise to hydrolytic decomposition of carbonates owing to alternating cycles of high-temperature hydrolysis and the thermal dehydration of the resulting hydroxides. Clearly, the presence of H_2O vapor and CO_2 during Li_2CO_3 thermolysis will favor Li_2O volatilization, most likely, in the form of LiOH [17]. The lithium losses from the $x = 0.17$ sample of system I after annealing (in both powder and compact forms) constitute 75–80% of the total lithium loss (Table 1, samples *3*–*5*). The choice of the annealing temperature and duration (1320 K, 2 h) was dictated by the conditions under which the fraction of the perovskite phase was at least 60–70%. Figure 3 shows the XRD patterns of samples I ($x = 0.17$) after annealing in the form of powder (scan *1*) and a compact (scan *2*). The yield of the perovskite phase evaluated from the XRD data is ≃65 and 80%, respectively, and the lithium losses are 20 and 21% (Table 1). Figure 4 displays the XRD patterns of sample I ($x = 0.17$) calcined at 1420 K for various lengths of time, and Fig. 5 shows the time and composition dependences of the perovskite cell volume. In the range 5–60 min (Fig. 5a), the unit-cell volume decreases since the lithium content of the forming perovskite phase rises. In contrast, at $\tau = 240$–300 min the unit-cell volume grows because of the lithium losses (Fig. 5a). At a sufficiently long heat-treatment time, the lithium losses from the single-phase sample (Fig. 4, scan *5*) lead to the formation of $LiNbO_3$ (scan *6*). According to Carruthers *et al.* [18], even long-term heat treatment of $LiNbO_3$ causes neither weight loss not changes in Curie temperature (which is known to be rather sensitive to Li stoichiometry [19]), which implies that there are no lithium losses. The present results lead us to conclude that lithium losses may result not only from Li_2CO_3 thermolysis but also—and, possibly, to a greater extent—from compositional changes in the perovskite phase. Clearly, the lithium loss during Li_2CO_3 thermolysis can be reduced by ensuring milder conditions for the formation of the intermediate Li-containing phases $LiMO_3$ and LiM_3O_8 [13, 16], which loose less Li [18] in comparison with Li_2O, subliming in the presence of H_2O and CO_2 [17]. Such conditions can be achieved using the following precursors:

(1) LiOH and coprecipitated $La(OH)_3$ and $M(OH)_5$;

(2) presynthesized $LaMO_4$, $LiMO_3$, and/or LiM_3O_8 (M = Nb, Ta);

(3) La_2O_3–Li_2CO_3–M_2O_5 (two-step annealing ensuring the formation of $LiMO_3$ and LiM_3O_8 at a low temperature (≃970 K) [13, 16] and the formation of the perovskite phase (at least 60%) at 1320 K).

The lithium loss from the Li-containing perovskite can be partially compensated for by adding an excess of Li into the starting mixture or by sintering samples

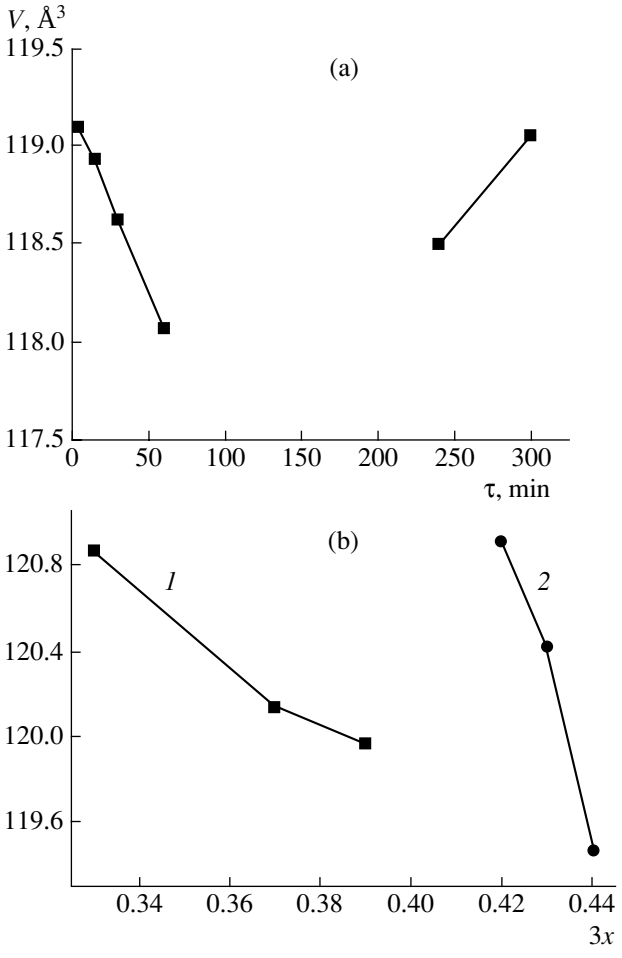

Fig. 5. Unit-cell volume of the cation-deficient perovskite phase as a function of (a) heat-treatment time and (b) lithium content for a sample of nominal composition $La_{0.5}Li_{0.5}Nb_2O_6$; (*1*) preset excess of Li, (*2*) different precursors (see Table 2).

packed with fired powder of the same composition [4]. The latter approach, however, requires increased amounts of expensive raw materials and does not fully prevents lithium losses [4].

Table 2 illustrates the effect of synthesis conditions on the lithium content of ceramics I and II with the nominal composition $x = 0.17$. The actual Li content of the ceramics correlates well with the composition dependence of the perovskite cell volume for a number of samples containing excess lithium (Fig. 5b, curve *1*; Table 2, samples *3–5*; Li excesses of 15, 33, and 45%, respectively) and prepared from different precursors (Fig. 5b, curve *2*; Table 2, samples *6–8*). It follows from the data in Table 2 that the presence of excess Li does not reduce Li losses as compared to conventional SRs. The HC process reduces lithium losses (by a factor of 4) only in system II (Table 2, samples *1*, *2*, *9*, *10*). TRs ($0.5LaNbO_4$–$0.5LiNbO_3$–$0.5Nb_2O_5$ precursor) reduce Li losses to 11 mol %, but the resulting ceramics are brittle and have a low density (sample *7*). The lithium losses can be reduced to 14–15 mol %, while maintaining a high density of the ceramic (5.2 g/cm^3 against ρ_x = 5.25 g/cm^3), using two-step SRs ($0.25La_2O_3$–$0.25Li_2CO_3$–Nb_2O_5) or TRs ($0.5LaNbO_4$–$0.5LiNb_3O_8$ precursor) (Table 2, samples *6*, *8*).

The Li loss data for systems I and II ($x = 0.17$) demonstrate that, in system II, the Li losses from the samples prepared by SRs and HC are lower by a factor of 1.7–2 and 6, respectively, than those from the corresponding samples in system I (Table 1, samples *3*, *7*; Table 2, samples *9*, *10*). Since the T_{sint} in system II is 250–300 K higher than that in system I [12], one might

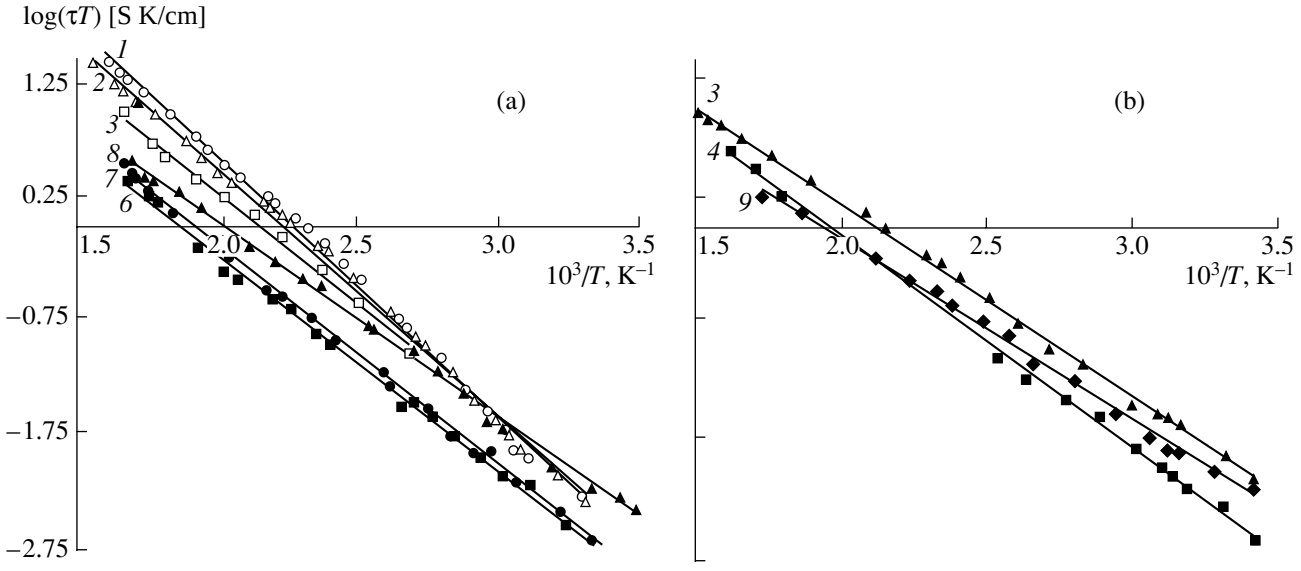

Fig. 6. Temperature dependences of conductivity for samples of nominal composition $La_{0.5}Li_{0.5}Nb_2O_6$ synthesized by different procedures (different lithium contents of the samples); the numbers at the curves identify the samples as referenced in Table 2.

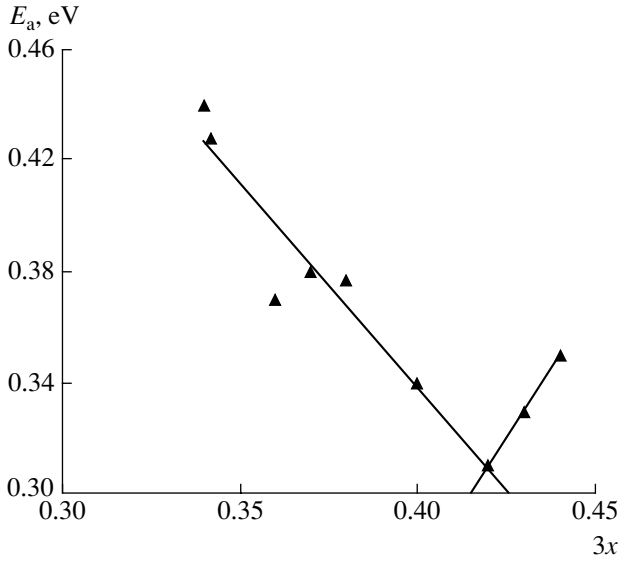

Fig. 7. Composition dependence of the activation energy for ionic conduction in samples of nominal composition $La_{0.5}Li_{0.5}Nb_2O_6$ synthesized by different procedures (see Fig. 6 and Table 2).

expect the opposite relationship. The likely reason for this behavior is that solid solutions in systems I and II are formed by different mechanisms [13, 16].

Table 3. Structural parameters of $La_{0.56}Li_{0.32}Nb_2O_6$ in three models

Model	A	B	C (O(1) + O(2) vacancies)
Lattice parameters			
a, Å	3.906(1)	3.905(3)	3.9048(1)
b, Å	3.906(1)	3.907(3)	3.9082(1)
c, Å	7.8783(2)	7.8786(2)	7.8791(2)
V, Å^3	120.21(6)	120.22(9)	120.239(6)
Positional parameter *z*			
Nb	0.2598(2)	0.2596(2)	0.2599(2)
O(3) or O(4)	0.233(1)	0.233(1)	0.232(1)
Site occupancy			
La	0.56	0.602	0.580(4)
Li	0.320	0.193	0.193
Nb	2.000	2.000	2.000
O(1)	1.000	1.000	0.93(6)
O(2)	1.000	1.000	0.91(6)
O(3)	2.000	2.000	2.000
O(4)	2.000	2.000	2.000
Reliability factor			
R_b, %	8.99	8.02	7.72
R_f, %	6.68	6.11	6.12

The preparation of solid solutions in systems I and II by SRs involves the formation of the intermediate phases $LaNbO_4$, $LiNbO_3$, and $LiNb_3O_8$ [13],

$$LaNbO_4 + LiNb_3O_8 \xrightarrow{1270\text{–}1470\ K} 2La_{0.5}Li_{0.5}Nb_2O_6,$$

and La_3TaO_7, $LaTaO_4$, $LaTa_3O_9$, $LaTa_5O_{14}$, $LiTaO_3$, and $LiTa_3O_8$ [16]

$$LaTa_3O_9 + LiTaO \xrightarrow{1470\text{–}1770\ K} 2La_{2/3-x}Li_{3x}Ta_2O_6,$$

respectively. During synthesis in system II, the Li-free perovskite-related phase $LaTa_3O_9$ is formed first and then reacts with $LiTaO_3$ (in contrast to syntheses in system I, where a Li-containing perovskite is formed in one step), which seems to reduce Li volatilization (Table 1, samples *3*, *7*). Using the HC process in system I, we obtained, in addition to the above intermediate phases, La_3NbO_7 and an *X* phase. The large number of intermediate phases impedes the formation of the perovskite phase, increasing the overall reaction time, despite the high reactivity of the coprecipitated hydroxides (Table 2, sample *9*). In system II, the mechanisms underlying the formation of solid solutions via SRs and HC are very similar. The high reactivity of the coprecipitated hydroxides substantially reduces the onset and endpoint temperatures of perovskite formation (by 250 and 100 K, respectively, compared to SRs) and lithium losses (by a factor of 4) (Table 2, samples *5*, *10*).

Li nonstoichiometry disturbs electroneutrality in $La_{2/3-x}Li_{3x}\square_{4/3-2x}M_2O_6$. The excess negative charge is neutralized via the formation of oxygen vacancies, as confirmed by structure refinement using the Rietveld profile analysis method for the sample with a nominal composition of $La_{0.56}Li_{0.32}Nb_2O_6$ and an actual lithium content $3x = 0.193$ (Table 3). As the initial approximation, we used model A (nominal site occupancies). The Li site occupancy in model B was inferred from chemical analysis data, and the La site occupancy was taken to suit the electroneutrality condition. In the next step, we refined the La and O site occupancies (model C). In the perovskite-related structure in question, oxygen sits in four positions: O(1) (1*f*: 1/2 1/2 0), O(2) (1*h*: 1/2 1/2 1/2), O(3) (2*s*: 1/2 0 *z*), and O(4) (2*r*: 0 1/2 *z*) (Fig. 1). In connection with this, we tested several combinations of site occupancies. The smallest *R*-factor was achieved in model C, with oxygen vacancies in positions O(1) and O(2). Thus, the oxygen vacancies sit in the same layers as the cation vacancies and Li ions (Fig. 1, positions 1*a*, 1*c*).

Figure 6 shows the temperature dependences of conductivity for ceramics with a nominal composition of $La_{0.5}Li_{0.5}Nb_2O_6$ and different actual Li contents. These data were used to assess the activation energy E_a of conduction. The plot of E_a versus $3x$ (Fig. 7) shows a minimum corresponding to $\square/3x \simeq 2.6$ and $\square/N \simeq 1.2$ (where *N* is the total number of A-site cations per formula unit). Clearly, the optimal lithium ion conductivity is offered by $La_{2/3-x}Li_{3x}\square_{4/3-2x}Nb_2O_6$ solid solutions

with $3x \simeq 0.41$–0.43 (±0.01 given the accuracy of atomic absorption analysis), or $x = 0.136$–0.143, prepared by two-step SRs (4 h at 970 K + 1.5 h at 1320 K) or TRs with the use of $LaNbO_4$ and $LiNb_3O_8$ as precursors (Table 2, samples *6*, *8*). These procedures appears attractive for controlled synthesis of Li-containing lanthanum metaniobate.

CONCLUSIONS

We studied the effects of the nominal composition and synthesis conditions on the lithium nonstoichiometry of $La_{2/3-x}Li_{3x}\square_{4/3-2x}Nb_2O_6$ (I) and $La_{2/3-x}Li_{3x}\square_{4/3-2x}Ta_2O_6$ (II) solid solutions. Our results demonstrate that, with increasing Li content, the Li losses relative to the nominal composition decrease. In solid-state synthesis, Li volatilizes mainly during Li_2CO_3 thermolysis in the starting mixture and the formation of a Li-containing cation-deficient perovskite phase. By optimizing the process conditions, lithium losses can be reduced from 26–30 (SRs) to 14–15 mol % (TRs) in system I ($x = 0.17$) and from 15 (SRs) to 4 mol % (HC) in system II. The Li losses from samples prepared by SRs and HC in system II are lower by a factor of 1.7–2 and 6, respectively, than those from the corresponding samples in system I, which suggests that solid solutions in these systems are formed by different mechanisms. Li nonstoichiometry disturbs electroneutrality in the solid solutions. The excess charge is neutralized via the formation of oxygen vacancies in positions O(1) (1*f*: 1/2 1/2 0) and O(2) (1*h*: 1/2 1/2 1/2). The optimal lithium ion conductivity is offered by solid solutions with $\square/3x \simeq 2.6$ and $x \simeq 0.136$–0.143.

REFERENCES

1. Belous, A.G., Novitskaya, G.N., Polyanetskaya, S.V., and Gornikov, Yu.I., Properties of $La_{2/3-x}Li_{3x}TiO_3$ Oxides, *Izv. Akad. Nauk SSSR, Neorg. Mater.*, 1987, vol. 23, no. 3, pp. 470–472.
2. Emery, G., Buzare, G.Y., Bohnke, O., and Fourquet, G.L., Lithium-7 NMR and Ionic Conductivity Studies of Lanthanium Lithium Titanate Electrolytes, *Solid State Ionics*, 1997, vol. 99, pp. 41–51.
3. Bohnke, O., Bohnke, C., and Fourquet, G.L., Mechanism of Ionic Conduction and Electrochemical Intercalation of Li^+ into the Perovskite Lanthanium Lithium Titanate, *Solid State Ionics*, 1996, vol. 91, pp. 21–31.
4. Mirumoto, K. and Hayashi, S., Conductivity Relaxation in Lithium Ion Conductors with the Perovskite-Type Structure, *Solid State Ionics*, 2000, vol. 127, pp. 241–251.
5. Mirumoto, K. and Hayashi, S., Lithium Ion Conduction in A-Site Deficient Perovskites $R_{1/4}Li_{1/4}TaO_3$ (R = La, Nd, Sm, and Y), *Solid State Ionics*, 1999, vol. 116, pp. 263–269.
6. Garsia-Martin, S., Royo, J.M., Tsukamoto, H., *et al.*, Lithium-Ion Conductivity in the Novel $La_{1/3-x}Li_{3x}NbO_3$ Solid Solution with Perovskite-Related Structure, *Solid State Ionics*, 1999, vol. 116, pp. 11–18.
7. Shan, Y.J., Sinozaki, N., and Nakamura, T., Preparation and Characterizations of New Perovskite Oxides $La_xNa_{1-3x-y}Li_y\square_{2x}NbO_3$ ($0.0 \le x$ and $y \le 0.2$), *Solid State Ionics*, 1998, vol. 108, pp. 403–406.
8. Garcia-Alvarado, F., Varez, A., Moran, E., and Alario-Franco, M.A., Structural Details and Lithium Intercalation in the Perovskite $La_{0.5}Li_{0.5}TiO_3$, *Phase Transitions*, 1996, vol. 58, pp. 111–120.
9. Rooksby, H.P., White, E.A.D., and Langston, S.A., Perovskite Type Rare-Earth Niobates and Tantalates, *J. Am. Ceram. Soc.*, 1965, vol. 48, pp. 447–449.
10. Belous, A.G., Gavrilenko, O.N., Pashkova, E.V., and Mirnyi, V.N., Lithium Ion Conductivity and Crystal Chemistry of $La_{2/3-x}Li_{3x}\square_{4/3-2x}Nb_2O_6$ Perovskite-Related Solid Solutions, *Elektrokhimiya*, 2002, vol. 38, no. 4, pp. 479–484.
11. Gavrilenko, O.N., Belous, A.G., Pashkova, E.V., and Mirnyi, V.N., Structural and Transport Properties of $La_{2/3-x}Li_{3x}\square_{4/3-2x}Ta_2O_6$ Perovskite-like Solid Solutions, *Neorg. Mater.*, 2002, vol. 38, no. 9, pp. 1126–1130 [*Inorg. Mater.* (Engl. Transl.), vol. 38, no. 9, pp. 949–953].
12. Belous, A., Pashkova, E., Gavrilenko, O., *et al.*, Lithium Ion-Conducting Materials Based on Complex Metaniobates and Metatantalates $La_{2/3-x}Li_{3x}\square_{4/3-2x}$ [Nb]Ta_2O_6 with Defect-Perovskite Structure, *Ionics*, 2002, vol. 9, pp. 21–27.
13. Belous, A.G., Pashkova, E.V., Gavrilenko, O.N., *et al.*, Heat-Treatment-Induced Phase Transformations in the Li_2CO_3–La_2O_3–Nb_2O_5 System, *Ukr. Khim. Zh.*, 2000, vol. 66, pp. 37–41.
14. *Certificate of Analysis: Standard Reference Material 1976, Instrument Sensitivity Standard for X-ray Powder Diffraction*, Gaithersburg: National Inst. of Standards and Technology, 1991, pp. 1–4.
15. Knipovich, Yu.N. and Morachevskii, Yu.V., *Analiz mineral'nogo syr'ya* (Analysis of Mineral Raw Materials), Leningrad: Khimicheskaya Literatura, 1956.
16. Belous, A.G., Pashkova, E.V., Gavrilenko, O.N., *et al.*, Heat-Treatment-Induced Phase Transformations in the Li_2CO_3–La_2O_3–Ta_2O_5 System, *Ukr. Khim. Zh.*, 2001, vol. 67, pp. 69–74.
17. Plyushchev, V.E. and Stepin, B.D., *Khimiya i tekhnologiya soedinenii litiya, rubidiya i tseziya* (Chemistry and Technology of Lithium, Rubidium, and Cesium Compounds), Moscow: Khimiya, 1970.
18. Carruthers, I.P., Peterson, G.E., Crasso, M., and Bridenbaugh, P.M., Nonstoichiometry and Crystal Growth of Lithium Niobate, *J. Appl. Phys.*, 1971, vol. 42, no. 5, p. 1846.
19. Palatnikov, M.N., Sidorov, N.V., Skiba, V.I., *et al.*, Effects of Nonstoichiometry and Doping on the Curie Temperature and Defect Structure of Lithium Niobate, *Neorg. Mater.*, 2000, vol. 36, no. 5, pp. 593–598 [*Inorg. Mater.* (Engl. Transl.), vol. 36, no. 5, pp. 489–493].